Renormalization of the phase transition in lead phosphate, $Pb_3(PO_4)_2$, by high pressure: structure

2001 J. Phys.: Condens. Matter 13 5353

(http://iopscience.iop.org/0953-8984/13/22/325)

INSTITUTE OF PHYSICS PUBLISHING JOURNAL OF PHYSICS: CONDENSED MATTER

J. Phys.: Condens. Matter **13** (2001) 5353–5364 www.iop.org/Journals/cm PII: S0953-8984(01)22703-9

Renormalization of the phase transition in lead phosphate, $Pb_3(PO_4)_2$, by high pressure: structure

R J Angel[1,4], **U Bismayer**[2] **and W G Marshall**[3]

[1] Bayerisches Geoinstitut, Universität Bayreuth, D-95440 Bayreuth, Germany
[2] Mineralogisch-Petrographisches Institut der Universität Hamburg, Grindelallee 48, D-20146 Hamburg, Germany
[3] ISIS Facility, Rutherford-Appleton Laboratory, Chilton, Didcot, Oxfordshire OX11 0QX, UK

E-mail: rangel@vt.edu

Received 7 March 2001

Abstract

The structure of the high-pressure phase of lead phosphate, $Pb_3(PO_4)_2$, has been determined from neutron powder time-of-flight diffraction data. Rietveld refinement to data collected at a pressure of 1.93(1) GPa and room temperature yielded unit-cell parameters $a = 5.4613(3)$ Å, $c = 20.069(1)$ Å, $V = 518.41(4)$ Å^3. The space group is $R\bar{3}m$. The structure consists of PO_4 tetrahedra together with Pb atoms in two symmetrically distinct sites. Analysis of the anisotropic displacement parameters of the Pb and O atoms indicates that they are spatially disordered within the structure. A structural model including split sites for these atoms suggests that the local environments around the Pb atoms in the high-pressure phase are very similar to those found in the low-pressure phase. We conclude that the phase transition from $C2/c$ to $R\bar{3}m$ symmetry occurs as a result of the disordering of the static displacements of the Pb2 atoms and not, to pressures of 1.93 GPa, as the result of the elimination of these displacements. The evolution of the structure of the monoclinic phase of lead phosphate with pressure was also followed. With increasing pressure there is an apparent decrease in the displacements of the Pb atoms from the symmetry points of the high-pressure phase, but that of Pb2 does not extrapolate to zero at the phase transition pressure.

1. Introduction

Lead phosphate, $Pb_3(PO_4)_2$, is an improper ferroelastic material that is a prototype for a large class of ferroelastics. It undergoes a phase transition from a high-temperature structure with trigonal $R\bar{3}m$ symmetry to a low-temperature phase with monoclinic $C2/c$ symmetry. Three orientation states, i.e. ferroelastic domains, are symmetry-allowed in the monoclinic

[4] Current address: Crystallography Laboratory, Department of Geological Sciences, Virginia Polytechnic and State University, Blacksburg, Virginia 24060, USA. Tel: 001-540-231-7974, Fax: 001-540-231-3386.

0953-8984/01/225353+12$30.00

ferrophase. In the monoclinic phase the trigonal symmetry is broken by displacements of Pb atoms from the triad axes, together with concomitant rotations and distortions of the PO_4 tetrahedra so as to provide appropriate coordination environments for the two symmetrically distinct Pb atoms within the structure. The transition is weakly first-order in character, with a cross-over close to the transition temperature into a regime in which the critical exponent of the order parameter is very close to the value expected for a three-states Potts model (0.2365) [1].

The application of pressure to lead phosphate at room temperature leads to the same symmetry change from monoclinic to trigonal at ∼1.8 GPa [2, 3]. The evolution of the spontaneous strain at high pressures indicates that the critical exponent is renormalized to a value close to $\frac{1}{2}$ [3] compared to the high-temperature phase transition. A further observation was that, in nominally hydrostatic pressure media, single crystals of lead phosphate undergo spontaneous twinning at pressures in excess of ∼1.3 GPa and that the spatial scale of this twinning decreases with increasing pressure up until the phase transition [3]. Previous single-crystal X-ray intensity data collected at 1.816(4) GPa indicated that the space group of the high-pressure phase is $R3m$ or $R\overline{3}m$ [3], and that its structure was very similar to that of the monoclinic phase. But the combination of the poor resolution of the data along the *c*-axis (due to the restricted access caused by the diamond-anvil cell) and the relatively weak scattering power of the oxygen atoms compared to the Pb atoms prevented a full structure refinement. We have therefore collected neutron powder diffraction data from samples of lead phosphate at pressures up to 1.8 GPa in order to determine the evolution of the structure towards the high-pressure phase transition, and therefore the structural basis for the behaviour previously observed. In addition a dataset collected just above the phase transition has allowed the structure of the high-pressure phase to be determined.

2. Experimental details

Two samples were synthesized from a stoichiometric mixture of PbO (Merck Art. 7401) and $(NH_4)H_2PO_4$ (Merck Art. 1126). In a first step the composition was heated to 720 K for 8 hours and secondly melted in a closed Al_2O_3 crucible. The melted lead phosphate was slowly cooled to room temperature and then powdered. The second sample was treated similarly in a closed platinum crucible and finally powdered again. The growth of related powders and single crystals has been described earlier [4].

Neutron powder diffraction data were collected on the HiPr instrument of the PEARL beamline at the ISIS facility, Oxfordshire, England. The instrument is a medium-resolution ($\Delta d/d \sim 0.008$ at $2\theta = 90°$), high incident flux neutron time-of-flight diffractometer [5]. Before each high-pressure run, each sample was loaded into a thin-walled cylindrical V can and a diffraction pattern was recorded at ambient conditions on the same instrument. High pressures were generated using a type V3b Paris–Edinburgh cell using standard profile WC/Ni-binder anvils which allow ∼90 mm^3 initial sample volume [6]. Pressures were determined from the unit-cell parameters of the sample through the equation of state previously determined by single-crystal x-ray diffraction [3]. Fluorinert (3M, grade FC75), which is usually employed as a low-scattering pressure medium in this cell, becomes non-hydrostatic at pressures below 1.4 GPa and the resulting non-hydrostatic stresses suppress the phase transition [2]. We therefore employed a 4:1 mixture by volume of deuterated methanol and deuterated ethanol as a pressure medium, because this mixture of hydrogenated alcohols remains hydrostatic to ∼10 GPa [7]. The peak widths of the diffraction maxima collected at the highest pressures attained in this experiment are identical to those obtained at ambient conditions, indicating that the deuterated mixture remains effectively hydrostatic to at least 1.9 GPa. Unfortunately,

use of this pressure medium resulted in the failure of one of the anvils of the pressure cell at approximately 2 GPa and only a single intensity dataset could be collected in the stability field of the high-pressure phase.

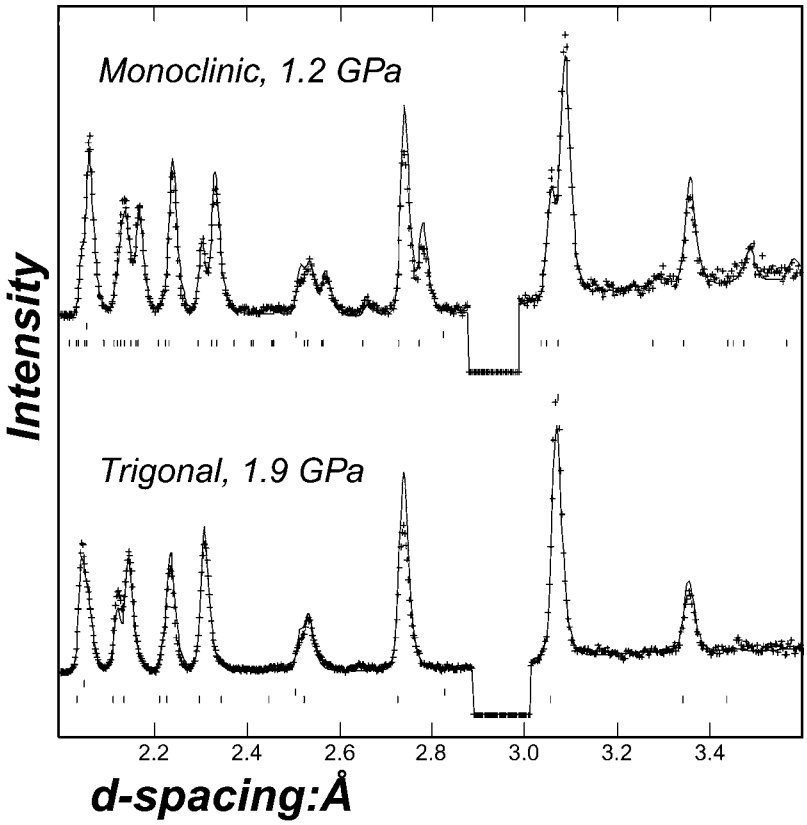

Figure 1. Typical neutron diffraction patterns of lead phosphate in the monoclinic (top) and trigonal (bottom) phases. Data is represented by the crosses and the refined patterns by the solid lines. Reflection markers are, from bottom, lead phosphate, WC and Ni. Note that the triplets of split reflections from the monoclinic phase (e.g. at ∼3.05 Å) become single sharp reflections in the diffraction pattern of the trigonal phase.

Data collection times at each pressure ranged between ∼30 minutes and 20 hours, the latter for the data collection from the high-pressure trigonal phase. The diffraction patterns (see figure 1) were obtained by electronic focusing of the individual detector element spectra, and normalization of the summed patterns with respect to the incident beam monitor and the scattering from a standard vanadium sample. Corrections were also made for the wavelength and scattering-angle dependence of the neutron attenuation by the anvil (WC) and gasket (TiZr) materials [8]. Rietveld refinements were performed with the GSAS program [9] to data with times-of-flight between 2.75 and 17.0 milliseconds, corresponding to *d*-spacings between 0.6 and 3.6 Å. In some patterns weak contamination from additional unidentified minor phases at large *d*-spacings was removed by excluding appropriate portions of the pattern from the refinement. At pressures below 1.2 GPa the peaks of the monoclinic phase of lead phosphate are sufficiently well resolved (figure 1) to allow the stable refinement of the profile parameters. At higher pressures, the evolution of the unit-cell metric towards trigonal symmetry means

that pairs of monoclinic peaks are no longer resolved and, as a result, the unit-cell parameters and the profile parameters of the lead phosphate cannot be refined simultaneously. In these cases, the profile parameters were fixed at the refined values obtained from lower pressure datasets. Positional parameters were refined for all atoms of the lead phosphate (table 1). Refinement of isotropic displacement parameters led to non-physical values in the monoclinic phase, so these were fixed at the values determined by single-crystal neutron diffraction [10]. Test refinements indicated that, provided they are chosen to be physically reasonable, the values of the isotropic displacement parameters do not significantly affect the values of the refined positional parameters. A March–Dollase function with one refineable parameter was used to correct the intensities for the preferred orientation arising from the dominant $(100)_{\text{mono}} \equiv (001)_{\text{trig}}$ cleavage of the material. The patterns also included diffraction maxima from the WC anvils of the pressure cell and from Ni which is present as a binder in the WC, so the scale, profile and unit-cell parameters of these phases were also refined.

Table 1. Refined structures of lead phosphate (sample S2).

	1 atm	0.29 GPa	1.15 GPa	1.44 GPa	1.66 GPa	1.80 GPa		1.93 GPa
Space group	$C2/c$	$C2/c$	$C2/c$	$C2/c$	C2/c	$C2/c$		$R\bar{3}m$
a (Å)	13.7990(6)	13.7862(12)	13.7593(9)	13.7494(14)	13.7456(14)	13.7407(16)		5.4614(3)
b (Å)	5.6917(3)	5.6555(6)	5.5526(5)	5.5230(8)	5.5002(8)	5.4893(9)		5.4614(3)
c (Å)	9.4196(4)	9.4204(9)	9.4310(7)	9.4340(11)	9.4347(11)	9.4313(13)		20.0697(12)
β (°)	102.359(6)	102.509(11)	102.926(9)	103.029(14)	103.100(15)	103.127(18)		
V (Å^3)	722.67(4)	717.05(9)	702.27(8)	697.95(12)	694.74(11)	692.78(12)		518.40(5)
Pb1 x	0	0	0	0	0	0	Pb1 x	0
y	0.2831(12)	0.281(3)	0.269(2)	0.264(4)	0.270(5)	0.261(6)	y	0
z	0.25	0.25	0.25	0.25	0.25	0.25	z	0
Pb2 x	0.3172(3)	0.3152(5)	0.3156(3)	0.3161(4)	0.3161(4)	0.3158(5)	Pb2 x	−0.0284(9)
y	0.3110(8)	0.3151(15)	0.3030(13)	0.296(3)	0.283(3)	0.282(4)	y	$-x$
z	0.3495(6)	0.3488(12)	0.3501(11)	0.3552(17)	0.3626(17)	0.362(3)	z	0.21034(17)
P x	0.6015(5)	0.6027(8)	0.6023(6)	0.6001(8)	0.6021(8)	0.6018(9)	P x	0
y	0.2582(16)	0.254(4)	0.266(3)	0.272(4)	0.268(6)	0.263(7)	y	0
z	0.4435(7)	0.4485(16)	0.4538(14)	0.4376(17)	0.4364(18)	0.438(2)	z	0.4020(4)
O1 x	0.4896(3)	0.4888(6)	0.4896(4)	0.4912(6)	0.4917(6)	0.4916(7)	O1 x	0.0217(13)
y	0.2276(11)	0.227(3)	0.261(3)	0.252(4)	0.245(5)	0.245(6)	y	$-x$
z	0.4189(8)	0.4166(17)	0.4093(12)	0.4260(16)	0.4310(15)	0.4305(18)	z	0.3273(3)
O21 x	0.6456(5)	0.6458(10)	0.6436(11)	0.6430(14)	0.6451(14)	0.642(3)	O2 x	−0.135(2)
y	0.0240(12)	0.021(3)	0.019(3)	0.022(4)	0.023(5)	0.017(5)	y	0.173(2)
z	0.3886(8)	0.3927(17)	0.3976(14)	0.386(2)	0.382(3)	0.380(4)	z	0.42890(14)
O22 x	0.6306(5)	0.6368(11)	0.6443(12)	0.6371(15)	0.6358(14)	0.641(3)		
y	0.4750(12)	0.473(3)	0.478(3)	0.471(4)	0.474(5)	0.468(5)		
z	0.3683(8)	0.3754(18)	0.3873(16)	0.371(3)	0.371(3)	0.374(4)		
O23 x	0.6419(5)	0.6405(9)	0.6385(7)	0.6473(11)	0.6475(12)	0.6480(14)		
y	0.2822(11)	0.289(3)	0.285(3)	0.268(4)	0.262(5)	0.264(6)		
z	0.6162(6)	0.6177(13)	0.6204(12)	0.6159(16)	0.6160(16)	0.615(2)		

Note. In the $R\bar{3}m$ structure, sites Pb2 and O1 have $\frac{1}{3}$ occupancy and the O2 site $\frac{1}{2}$ occupancy.

3. Results

The structural evolution of lead phosphate with increasing pressure is best discussed in the context of an idealized trigonal structure with $R\bar{3}m$ symmetry as found for Ba-phosphate and

Sr-phosphate at room conditions [11]. In these structures there are two symmetrically distinct large cation positions, one phosphate tetrahedron, and two distinct oxygen atoms (figure 2(a)). All of the atoms except O2 are located on the triad axes, and the tetrahedra are therefore constrained to have trigonal symmetry, with O1 being the apical atom on the triad. The O2 atoms occupy a special position x, $-2x$, yz on the $(1\bar{2}0)$ mirror planes, and three of them form the base of each tetrahedron which is therefore constrained to lie parallel to (001) of the trigonal unit cell (figure 2(a)). The two large cation positions have different coordination environments in this ideal structure. The Pb1 site is octahedrally coordinated by the O2 atoms, with a further 6 O1 atoms at distances greater than 3 Å (figure 3(a)). The Pb2 site is asymmetric, with a single short bond along the triad axis to an O1 oxygen, six approximately equatorial bonds to O2 atoms, and a further three longer bonds to O2 atoms on the side of Pb2 away from the short bond to O1 (figure 3(b)).

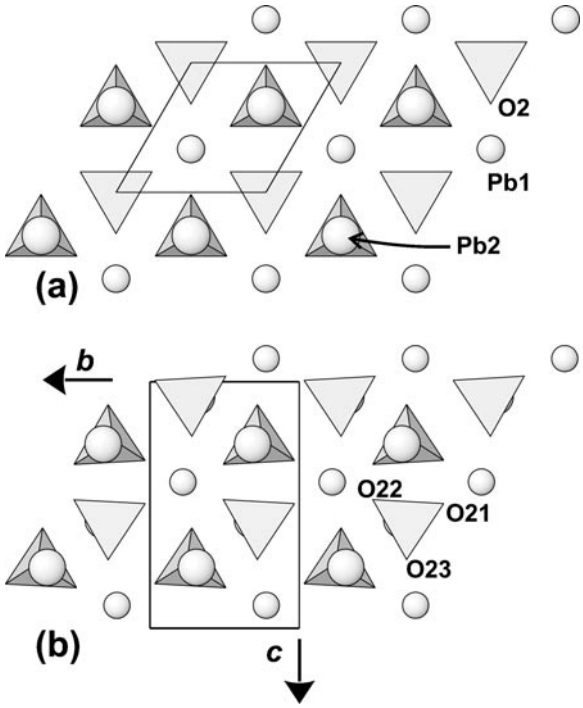

Figure 2. (a) Idealized trigonal structure of lead phosphate. The tetrahedra represent the PO_4 groups, small spheres Pb1 atoms and large spheres Pb2 atoms. Part (b) shows the monoclinic structure of lead phosphate at room temperature and pressure in the same orientation, projected onto $(100)_{mono}$.

3.1. Room pressure structure

In a single ferroelastic domain at room pressure and temperature the structure of lead phosphate is monoclinic [10, 12] due to the ordered displacements of both of the Pb atoms from the triad axes of the ideal trigonal structure (figure 2(b)). The breaking of the trigonal symmetry means that the PO_4 tetrahedra are no longer required to have 3-fold rotational symmetry. The O2 position of the trigonal structure therefore becomes three independent positions which we denote O21, O22, O23 (equivalent to O1, O2 and O3 of previous reports [10, 12]). In the

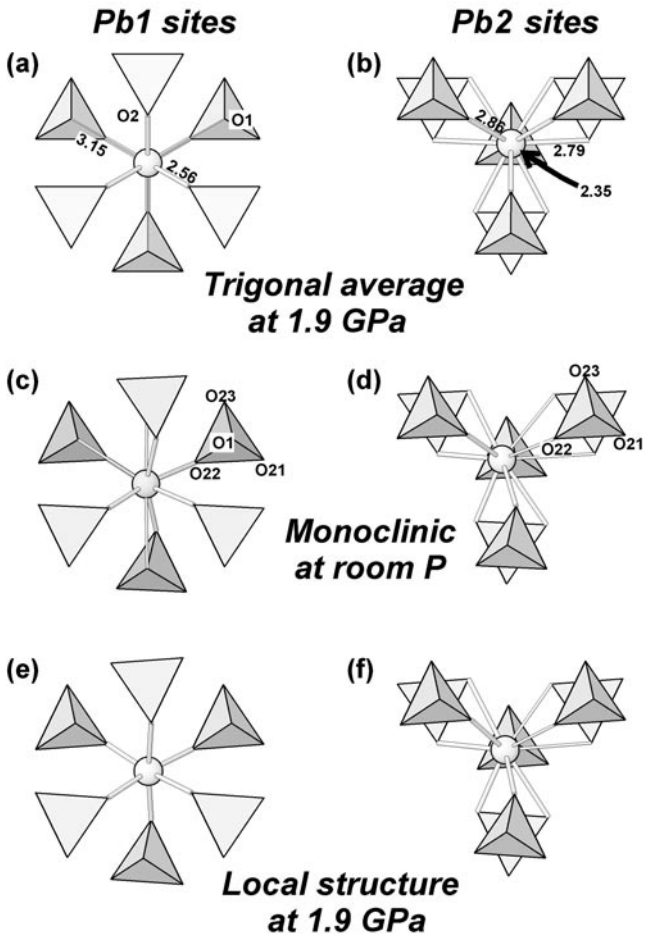

Figure 3. The local environments around the two Pb atoms under various conditions, as labelled. Note that the local structures in the trigonal structure at 1.9 GPa (e) and (f), are very similar to those in the monoclinic structure at room pressure (c) and (d).

monoclinic phase the PO_4 tetrahedra are slightly distorted from a perfect tetrahedral form, with the bond to the apical oxygen (O1) remaining shorter than the other three P–O bonds, and the O–P–O angles distorted by up to 4° from the ideal 109.5°. In addition, the PO_4 tetrahedra are both tilted so that the triangular face formed by the O21–O22–O23 oxygen atoms is not parallel to (100) of the monoclinic unit-cell, and rotated to provide better coordination to the displaced Pb atoms (figure 2(b)). The Pb1 site remains octahedrally coordinated with bond lengths ranging from 2.55 Å to 2.59 Å with a further three Pb1–O1 distances less than the Pb1–P distance (figure 3(c)). The Pb2 site exhibits a one-sided coordination of seven shorter bonds less than 3.0 Å with three longer bonds on the opposite side (figure 3(d)). This pattern of distortion, together with the bond valence sums at Pb2 being significantly less than 2, clearly indicates that the lone-pair of electrons on the Pb atom is sterically active [10, 13].

The bond lengths obtained from the refinements to our two room pressure datasets show some differences, but mostly lie within the bounds of two previous structure refinements [10, 12]. Some of these differences can be attributed to the presence of additional unrefined

minor phases in our sample S1, as well as differences between all four samples including possible oxygen deficiency [14], and the short times of our data collections. But all four refinements show the same pattern of displacements and distortions from the ideal trigonal structure.

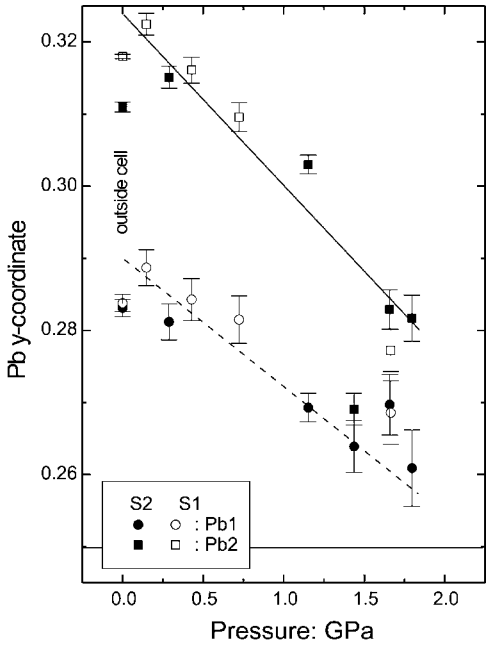

Figure 4. The evolution with pressure of the y-coordinates of the two Pb atoms. Lines are guides to the eye only. In the ideal trigonal structure the value of both coordinates would be $\frac{1}{4}$. Note that the Pb2 coordinate appears to extrapolate to $\frac{1}{4}$ at a pressure significantly above the phase transition.

3.2. Evolution of the monoclinic structure

The most significant change in the structure upon increasing pressure is the shift of the refined positions of both symmetrically independent Pb atoms towards the triad axes of the monoclinic phase (figure 4). While the displacement of Pb1 appears to extrapolate to zero in the region of the phase transition, it is clear that the displacement of Pb2 does not. Despite the large displacements of the Pb atoms (∼0.25 Å) there is no significant change in the average Pb–O distances, although the coordination environment of Pb2 becomes more regular, while the shortest Pb2–O bond to O1 remains unchanged within the uncertainties (figure 5). The data are not sufficiently precise to determine whether there are any significant changes to the geometry of the PO_4 tetrahedron, nor whether it undergoes significant rotation with increasing pressure. Of the four distinct distances between the Pb1 and Pb2 atoms, one decreases by 0.15 Å, and the remainder show no significant evolution with pressure; all remain greater than 3.95 Å. The Pb2 atoms are arranged in 'corrugated' or 'double' layers parallel to (100) of the monoclinic phase and (001) of the trigonal phase (figure 6). Within each layer, each Pb2 atom has three nearest neighbours, all of which are located in the other half of the layer. At room pressure the ordered displacements of the Pb2 atoms from the ideal trigonal positions leads to each Pb2 atom having two neighbours at a distance of 3.68 Å, and one at 3.77 Å. While

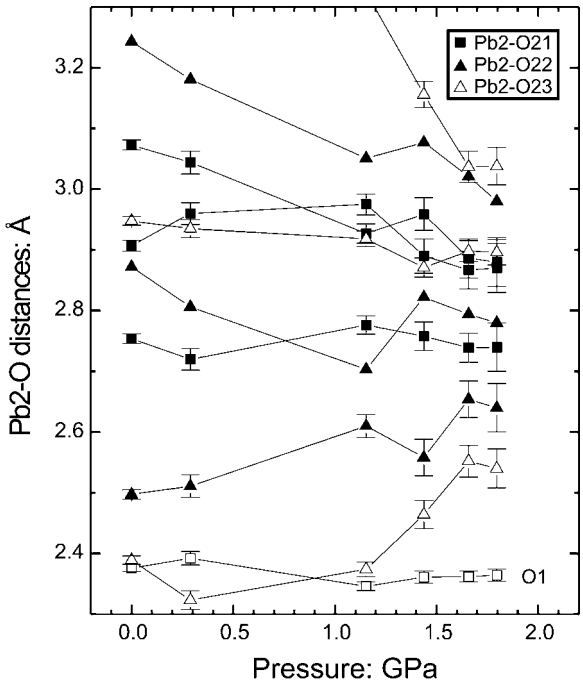

Figure 5. Variation of Pb2–O distances in the monoclinic phase from refinements to the S2 sample datasets.

the two shorter distances do not change significantly with pressure, the longer one apparently decreases to ∼3.5 Å on approaching the phase transition into the high-pressure phase (figure 7).

3.3. Structure of the high-pressure phase

Single-crystal x-ray diffraction studies determined the space group of the high-pressure phase of lead phosphate to be either $R3m$ or $R\bar{3}m$ [3]. The neutron powder diffraction data do not allow these two space groups to be distinguished, so space group $R\bar{3}m$ (corresponding to the high-temperature, room-pressure space group) was assumed throughout the refinements. An initial refinement with the atoms allocated to the symmetry positions of the ideal structure described above led to the structure illustrated in figures 3(a) and 3(b). This structure model leads to highly anisotropic displacement parameters for Pb2, with $U_{11} \sim 10U_{33}$, suggestive of positional disorder in the (001) plane, but displacement parameters for Pb1 that are isotropic within the uncertainties. An improved fit to the data was achieved with a model in which Pb1 remains on the triad, but Pb2 is displaced to a set of split-atom sites $-x, x, z$ (each $\frac{1}{3}$ occupancy). The displacement parameters of O1 and O2 also appear to be strongly anisotropic, with U_{33} refining to negative values in both cases, so these were also refined as split sites at $-x$, x, z and x, y, z respectively and their displacement parameters constrained to be isotropic and equal. This choice of split positions provides the physically most reasonable structural model (table 1) that in fact provides the best fit to the data that we were able to obtain, and a significantly better fit than that of the ideal trigonal structure.

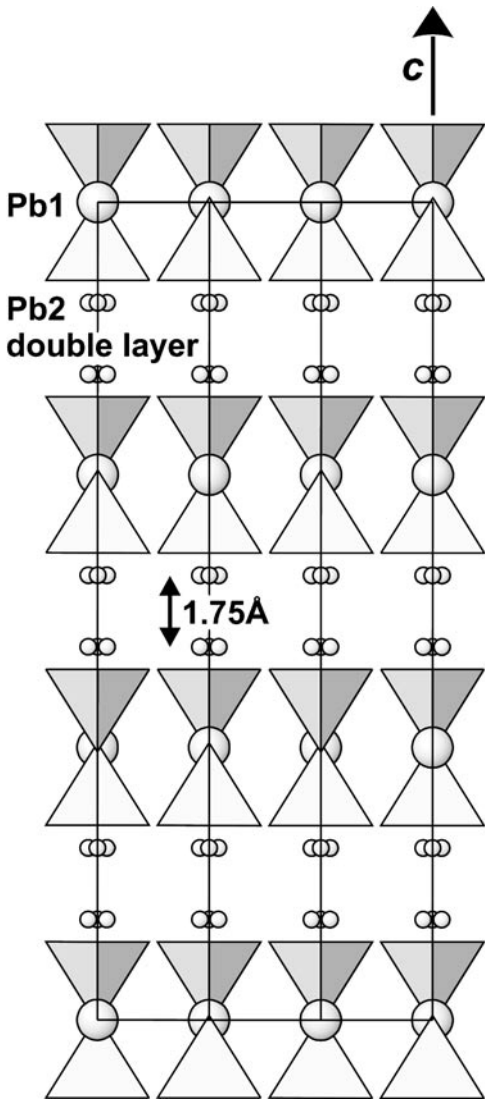

Figure 6. Structure of the trigonal phase of lead phosphate at 1.9 GPa, viewed down $(100)_{trig}$. The Pb2 atoms are shown as three-fold split sites.

4. Discussion

The refined structure of the trigonal high-pressure phase (table 1) represents a spatial average of several statically distorted local environments with the displacements disordered on a long-range length scale, as has also been found for Ba-doped $Pb_3(PO_4)_2$ [15]. The alternative of dynamically-disordered displacements such as those found at high temperatures just above T_c seems physically unreasonable at pressures in excess of those at which a statically-ordered monoclinic phase is stable. In other words, pressure leads to the condensation of the dynamically-disordered displacments observed in the intermediate phase just above T_c at room pressure [16].

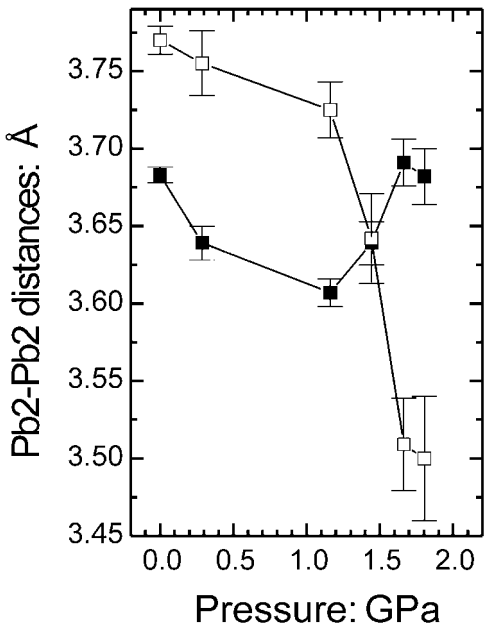

Figure 7. Evolution of Pb2–Pb2 distances with pressure in the monoclinic phase of lead phosphate, determined from refinements to the S2 sample datasets.

Although the local structure cannot be uniquely determined from such an average, possible local environments around the Pb sites can be derived by making a choice between the split-atom sites of the average model. We start by assuming that the strongly-bonded PO_4 tetrahedron does not undergo large internal distortions. Because the P atom remains on the triad axis, this implies that the major local deviation from the average symmetry imposed by the $R\bar{3}m$ space group must be a rotation of the tetrahedron. This in turn allows one to select one subset of the split O2 atom positions as one of the local configurations; the resulting P–O2 bond lengths and O2–P–O2 angles are the same as those in the trigonal average structure. The split site for the O1 atom indicates that a small distortion of the tetrahedron does occur. This is presumably due to sterical reasons including the need to maintain reasonable P–O1 and O1–Pb2 distances, despite the Pb2–P distance being ∼0.1 Å shorter in the trigonal average structure at 1.93 GPa than at room pressure.

These local configurations of tetrahedra can then be used to construct physically reasonable local environments around the two symmetrically distinct Pb atoms. Because the Pb1 remains on the triad axis (within experimental uncertainties), the Pb1–O bond lengths remain unchanged from the trigonal average structure, but there is a slight distortion (1–2°) of the O–Pb1–O bond angles. All of the shorter Pb1–O2 bonds in the local structure at 1.93 GPa are 2.56 Å, only 0.02 Å shorter than the average in the room-pressure structure. The four longer Pb1–O1 bonds are 3.06 Å in the local structure of the high-pressure phase compared to 3.01(1) and 3.10(1) Å in the room-pressure structure. These results suggest that the local environment around the Pb1 site is essentially the same in the high-pressure phase as in the monoclinic phase at room pressure (figure 3(e), 3(c)).

Because the Pb2 site is refined as a split-atom site in the high-pressure phase, a number of local configurations can be derived from different choices of tetrahedral rotations and Pb2 displacements. The configuration shown in figure 3(f) is the one with the most physically

likely bond lengths. Of particular note is that this combination of displacements of Pb2 and O1 increases the shortest Pb2–O1 bond length from 2.35 Å in the trigonal average structure to a value of 2.40 Å, similar to the 2.39 Å found at room pressure. The general pattern of one-sided coordination is very similar to that found in the monoclinic phase at room pressure (figure 3(d)), and the average of the seven shorter Pb2–O bonds is the same as at room pressure. However, the three longer Pb2–O contacts appear to be significantly shortened by between ∼0.15 Å and ∼0.3 Å.

The preceding examination of the refined structure of the high-pressure phase suggests that both the PO_4 tetrahedra, and the local environments, around the Pb atoms are very similar to those found in the room-pressure structure with the exception that the Pb1 atom apparently lies on, or very close to, the triad axis. This is what would be expected from the pressure evolution of the Pb1 position within the monoclinic phase, which extrapolates to the triad axis in the region of the pressure-induced phase transition (figure 4). The fact that the Pb2 displacement does not extrapolate to zero at the phase transition is consistent with the presence of a static disordered displacement of these atoms in the high-pressure phase.

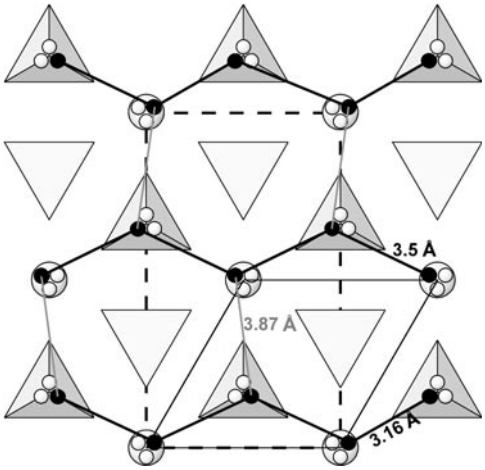

Figure 8. The structure of one double-layer of Pb2 atoms in the trigonal phase at 1.9 GPa, with the Pb2 atoms shown as three-fold split sites. If 3.16 Å contacts between Pb2 atoms are forbidden then, on average, each Pb2 atom has two Pb2 neighbours at ∼3.5 Å and one at ∼3.87 Å. The ordered pattern of displacements corresponding to that found in the monoclinic phase is indicated by the filled circles and leads to the larger unit-cell indicated by the dashed lines.

The evolution of the distances between the Pb2 atoms within the structure suggests a possible mechanism for both the structural evolution in the monoclinic phase, and for the scale and organization of the disorder in the high-pressure phase. In contrast to the arrangement in the monoclinic phase, within the high-pressure phase the distances between the split-atom positions yield two short Pb2–Pb2 distances of ∼3.5 Å and one longer one of 3.87 Å from each Pb2 (figure 8). Any arrangement of Pb2 displacements within a double layer that excludes short Pb2–Pb2 distances of 3.16 Å (figure 8) yields the same average of two short and one long Pb2–Pb2 distance. Disordering of the Pb2 displacements within the structure at high pressures could then be due to one of two mechanisms. Either the displacements become disordered within the double layers, or the correlation between the successive (001) double layers is lost. The former would require energetically unfavourable distortions of the PO_4 tetrahedra, rather than rotations. The linkages between successive Pb2 layers are, however, indirect and involve Pb2–Pb1 linkages. Therefore, the coupling between successive Pb2 double layers is expected

to be weaker than the interactions between the Pb2 atoms within the layers. The additional observation that the Pb1 atoms apparently occupy positions on the triad axes in the trigonal structure suggests that the second model, of loss of correlation of displacements between layers within each of which a monoclinic ordering pattern is retained, is the more likely one.

The observation of diffuse super-lattice reflections elongated perpendicular to the Pb double-layers [17, 18] suggests that a similar mechanism occurs in the monoclinic phase on increasing temperature. Then the ferroelastic transition from the monoclinic to the trigonal phase results, on an atomistic scale, from the loss of correlation of ordering between the layers because the interactions between layers are weaker than within the layers. This first transition has a negative slope in P–T space [19, 20], and is, therefore, the same phase boundary that we have crossed in our high-pressure experiments. The further high-temperature phase transition at ∼530 K [21] at room pressure would then involve the complete loss of ordering within the double layers of Pb2 atoms. Whether the P–T slope of this second trigonal–trigonal transition is positive or negative has yet to be determined. But certainly no anomalies were detected in the unit-cell parameters of lead phosphate to ∼6 GPa at room temperature [3], which puts a minimum bound on the value of $\mathrm{d}P/\mathrm{d}T$ for the second, iso-symmetric, transition.

Acknowledgments

Neutron diffraction experiments were performed on the PEARL beamline of the ISIS facility with the support of the Central Laboratories Research Council (CLRC) and funded by the UK Engineering and Physical Sciences Research Council (EPSRC). The technical assistance of Mr D J Francis was greatly appreciated.

References

[1] Salje E K H and Devarajan V 1981 *J. Phys. C: Solid State Phys.* **14** L1029
[2] Decker D L, Peterson S, Debray D and Lambert M 1979 *Phys. Rev.* B **19** 3552
[3] Angel R J and Bismayer U 1999 *Acta Crystallogr.* B **55** 896
[4] Bismayer U and Salje E K H 1981 *Acta Crystallogr.* A **37** 145
[5] *ISIS Annual Report* 1996 ISSN 1358-6254
[6] Besson J M, Nelmes R J, Hamel G, Loveday J S, Weill G and Hull S 1992 *Physica B* **180–181** 907
[7] Eggert J H, Xu L, Che R, Chen L and Wang J 1992 *J. Appl. Phys.* **72** 2453
[8] Wilson R M, Loveday J S, Nelmes R J, Klotz S and Marshall W G 1995 *Nucl. Instrum. Meth.* A **354** 145
[9] Larsen A C and von-Dreele R B 1985 *Los Alamos National Laboratory Report* LAUR B6-748
[10] Kiat J M, Yamada Y, Chevrier G, Uesu Y, Boutrouille P and Calvarin G 1992 *J. Phys.: Condens. Matter* **4** 4915
[11] Sugiyama K and Tokonami M 1990 *Miner. J. Japan* **15** 141
[12] Ng H N and Calvo C 1975 *Can. J. Phys.* **53** 42
[13] Wang X and Liebau F 1996 *Z. Kristallogr.* **211** 437
[14] Bleser T, Berge B, Bismayer U and Salje E K H 1994 *J. Phys. C: Condens. Matter* **6** 2093
[15] Hensler J, Boysen H, Bismayer U andVogt T 1993 *Z. Kristallogr.* **206** 213
[16] Salje E K H, Devarajan V, Bismayer U and Guimaraes D M C 1983 *J. Phys. C: Solid State Phys.* **16** 5233
[17] Joffrin C, Benoit J P, Currat R and Lambert M 1979 *J. Physique* **40** 1185
[18] Bismayer U, Salje E K H and Joffrin C 1982 *J. Physique* **43** 1379
[19] Tolédano J C, Pateau L, Primot J, Aubrée J and Morin D 1975 *Mater. Res. Bull.* **10** 103
[20] Midorikawa M, Kashida H and Ishibashi Y 1981 *J. Phys. Soc. Japan* **50** 1592
[21] Salje E K H and Wruck B 1983 *Phys. Rev.* B **28** 6510